Biomedicine & Pharmacotherapy 167 (2023) 115548

Contents lists available at ScienceDirect

Biomedicine & Pharmacotherapy

journal homepage: www.elsevier.com/locate/biopha

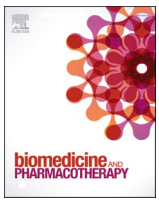

Inhibition of xanthine oxidase-catalyzed xanthine and 6-mercaptopurine oxidation by luteolin, naringenin, myricetin, ampelopsin and their conjugated metabolites

Orsolya Balázs [a,b], Ágnes Dombi [a], Balázs Z. Zsidó [c], Csaba Hetényi [c], Kateřina Valentová [d], Róbert G. Vida [b], Miklós Poór [a,*]

[a] Department of Pharmacology, Faculty of Pharmacy, University of Pécs, Rókus u. 2, H-7624 Pécs, Hungary
[b] Department of Pharmaceutics and Central Clinical Pharmacy, Faculty of Pharmacy, University of Pécs, H-7624 Pécs, Hungary
[c] Unit of Pharmacoinformatics, Department of Pharmacology and Pharmacotherapy, Medical School, University of Pécs, Szigeti út 12, H-7624 Pécs, Hungary
[d] Institute of Microbiology of the Czech Academy of Sciences, Vídeňská 1083, CZ-142 00 Prague, Czech Republic

ARTICLE INFO

Keywords:
Xanthine oxidase
Luteolin
Naringenin
Myricetin
Ampelopsin
Flavonoid conjugates

ABSTRACT

Luteolin, naringenin, myricetin, and ampelopsin are abundant flavonoids in nature, and several dietary supplements also contain them at very high doses. After the peroral intake, flavonoids go through extensive presystemic biotransformation; therefore, typically their sulfate/glucuronic acid conjugates reach high concentrations in the circulation. Xanthine oxidase (XO) enzyme is involved in uric acid production, and it also takes part in the elimination of certain drugs (e.g., 6-mercaptopurine). The inhibitory effects of flavonoid aglycones on XO have been widely studied; however, only limited data are available regarding their sulfate and glucuronic acid conjugates. In this study, we examined the impacts of luteolin, naringenin, myricetin, ampelopsin, and their sulfate/glucuronide derivatives on XO-catalyzed xanthine and 6-mercaptopurine oxidations employing in vitro enzyme incubation assays and molecular modeling studies. Our major results/conclusions are the following: (1) Sulfate metabolites were stronger while glucuronic acid derivatives were weaker inhibitors of XO compared to the parent flavonoids. (2) Naringenin, ampelopsin, and their metabolites were weak inhibitors of the enzyme. (3) Luteolin, myricetin, and their sulfates were highly potent inhibitors of XO, and the glucuronides of luteolin showed moderate inhibitory impacts. (4) Conjugated metabolites of luteolin and myricetin can be involved in the inhibitory effects of these flavonoids on XO enzyme.

1. Introduction

Luteolin (LUT), naringenin (NAR), myricetin (MYR), and ampelopsin (AMP) are flavonoid aglycones (Fig. 1); the parent flavonoids and/or their glycosides appear in numerous plants and plant-based products. Due to their supposed beneficial health effects, several dietary supplements contain high doses of LUT, NAR (or its 7-*O*-glucoside naringin), MYR, or AMP, leading to extremely high intake compared to the normal diet. The distributor's websites suggest the following effects of these dietary supplements (see the links of the websites and other details in the Supplementary): antioxidant (LUT, NAR, MYR, and AMP), immunity booster (LUT and NAR), anti-inflammatory (LUT and AMP), supporting cognitive health (LUT), liver support (AMP), and anti-hangover (AMP). The recommended daily doses based on the websites are typically 100 mg for LUT and MYR, 500 mg for NAR or naringin, and 300–600 mg for AMP (see in the Supplementary). Generally, flavonoids have low oral bioavailability resulting from their high presystemic biotransformation [1,2]. Therefore, typically their sulfate and/or glucuronide metabolites reach high concentrations in the systemic circulation (and likely in some tissues) [3]. Nevertheless, several research studies aim to improve the oral bioavailability of flavonoids, e.g., with special formulations or prodrug formation [4].

LUT is a flavone aglycone. Based on human studies, the peak plasma concentration of total LUT (the parent flavonoid and its metabolites) can exceed 1 μM (after peroral, single dose administration of 50 mg LUT) [5]. Nevertheless, in animal studies, large doses of LUT resulted in even 10 μM or higher plasma levels [6]. After the oral administration of LUT to human volunteers, its sulfate and glucuronide conjugates were

* Corresponding author.
E-mail address: poor.miklos@pte.hu (M. Poór).

https://doi.org/10.1016/j.biopha.2023.115548
Received 1 August 2023; Received in revised form 13 September 2023; Accepted 18 September 2023

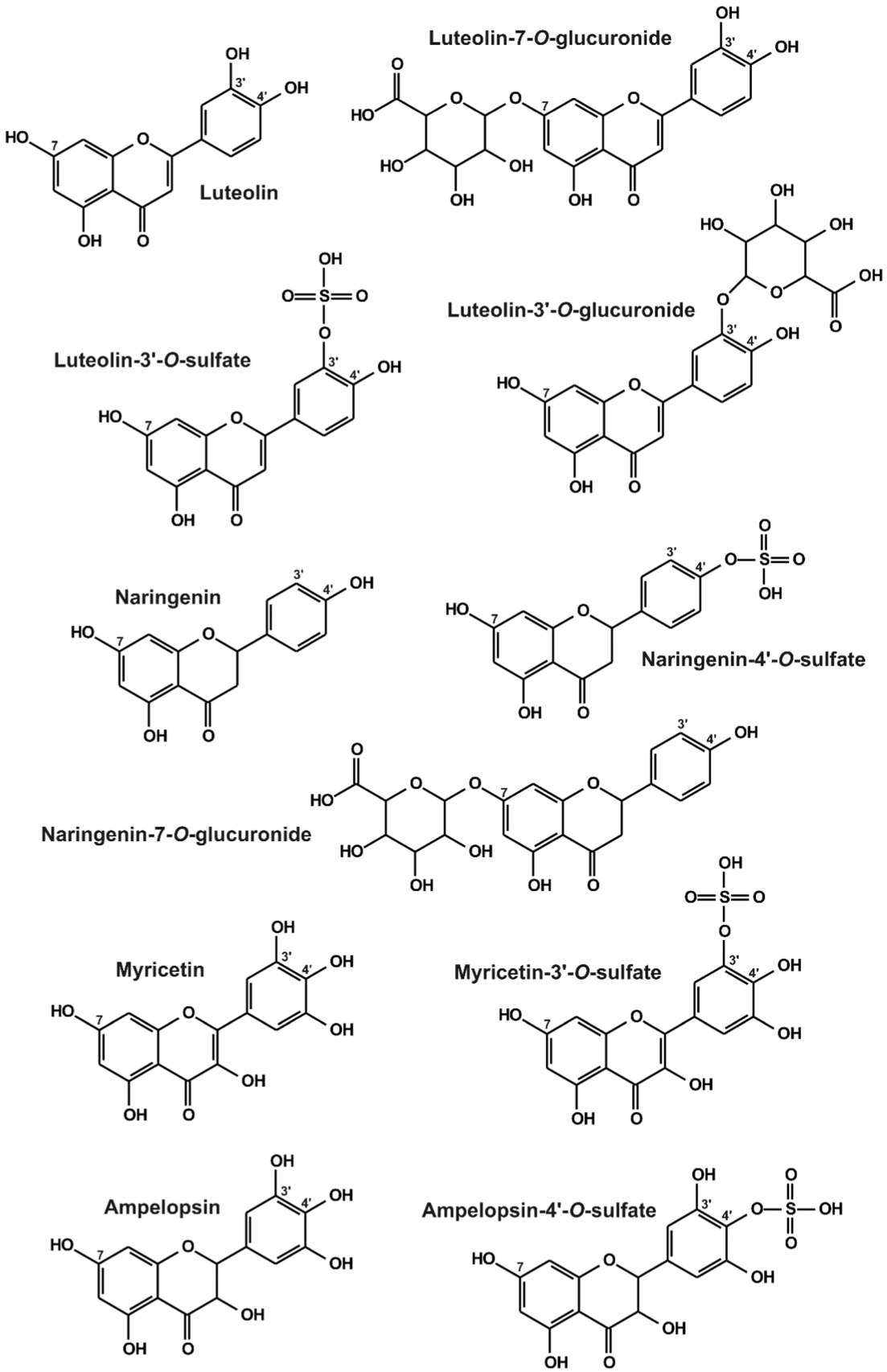

Fig. 1. Chemical structures of luteolin (LUT), luteolin-3′-*O*-sulfate (L3′S), luteolin-3′-*O*-glucuronide (L3′G), luteolin-7-*O*-glucuronide (L7G), naringenin (NAR), naringenin-4′-*O*-sulfate (N4′S), naringenin-7-*O*-glucuronide (N7G), myricetin (MYR), myricetin-3′-*O*-sulfate (M3′S), ampelopsin (AMP), and ampelopsin-4′-*O*-sulfate (A4′S).

identified in human plasma, and luteolin-3′-*O*-sulfate (L3′S) has been reported as the major circulating metabolite [7]. Furthermore, luteolin-3′-*O*-glucuronide (L3′G), luteolin-4′-*O*-glucuronide, and luteolin-7-*O*-glucuronide (L7G) were also detected in the plasma, liver, kidney, and small intestine samples of rats [7].

NAR is a flavanone aglycone, its sulfate and glucuronic acid metabolites can reach high concentrations in the human blood and urine [8,9]. In human studies, the peak plasma concentration (C_{max}) of total NAR was approximately 6 μM after the consumption of 8 mL/kg grapefruit juice [10]; and the single peroral doses (150 mg and 600 mg) of NAR led to 15.8 μM and 48.5 μM C_{max} values of total NAR, respectively [11]. In addition, micromolar concentrations of sulfate and glucuronic acid conjugates of NAR were found in rat liver samples [12].

MYR is a flavonol, while AMP (or dihydromyricetin) is a flavanonol aglycone. The oral bioavailability of MYR is low (approximately 10% in rats) [13]. After the peroral administration of MYR (100 mg/kg) to rats, the peak plasma concentration of total MYR (the parent flavonoid and its metabolites) was approximately 8 μM [13]. In rat studies, the oral bioavailability of AMP was 4% [14]. Nanomolar concentrations (approximately 300–500 nM) of AMP were detected in rats after the *per os* treatment with AMP (100 mg/kg) [15,16]. Nevertheless, it is reasonable to hypothesize that certain sulfate and/or glucuronide metabolites of MYR and AMP can reach micromolar concentrations in the circulation.

Xanthine oxidoreductase is a non-microsomal enzyme with molybdenum center, its two interconvertible forms are xanthine oxidase (XO) and xanthine dehydrogenase [17]. The latter can be reversibly or irreversibly converted to XO [18]. 6-Mercaptopurine (6-MP) and its prodrug azathioprine are widely applied drugs in the treatment of cancer and autoimmune diseases, including acute lymphoblastic leukemia, Crohn's disease, and ulcerative colitis [19]. XO can biotransform endogenous compounds (e.g., xanthine to uric acid) and certain drugs (e.g., 6-MP to 6-thiouric acid; Fig. 2). Therefore, the inhibition of the enzyme (e.g., with allopurinol) is beneficial in hyperuricemia due to the decreased uric acid formation [20], while it can cause life-threatening drug interaction resulting from the poor elimination of 6-MP [21]. Allopurinol and febuxostat are potent inhibitors of XO and are applied in the pharmacotherapy of hyperuricemia and gout [18]. Previous in vitro studies also demonstrated the highly potent inhibitory actions of flavonoids on the XO enzyme [20].

In in vitro investigations, LUT and MYR proved to be strong inhibitors of XO, while NAR and AMP caused moderate inhibition [22–24]. However, the impacts of their sulfate and glucuronic acid conjugates on the XO enzyme have not been examined yet. Previously, we reported that quercetin-3′-*O*-sulfate is a potent inhibitor of XO, even more potent than the parent flavonoid quercetin and the positive control inhibitor allopurinol [25]. In addition, most of the studies investigated the impacts of flavonoids on the XO-catalyzed xanthine oxidation, while their inhibitory effects on 6-MP oxidation have been barely characterized. It would be interesting because earlier studies highlighted that some polyphenols and even allopurinol show different inhibitory potency regarding xanthine vs. 6-MP oxidation [25,26], and the strong inhibition of XO during 6-MP treatment can have serious consequences [21].

In this study, we aimed to examine the interactions of LUT, NAR, MYR, AMP, and their sulfate/glucuronide conjugates with the XO enzyme. The inhibitory effects of LUT, L3′S, L3′G, L7G, NAR, naringenin-4′-*O*-sulfate (N4′S), naringenin-7-*O*-glucuronide (N7G), MYR, myricetin-3′-*O*-sulfate (M3′S), AMP, and ampelopsin-4′-*O*-sulfate (A4′S) were tested on XO-catalyzed xanthine and 6-MP oxidations, employing in vitro enzyme incubation assays. In both experiments, allopurinol was applied as positive control inhibitor. In addition, molecular modeling studies were also performed to explore the molecular bases of the inhibitory effects of the flavonoids tested. Our results demonstrate that some of the conjugated metabolites are highly potent inhibitors of XO.

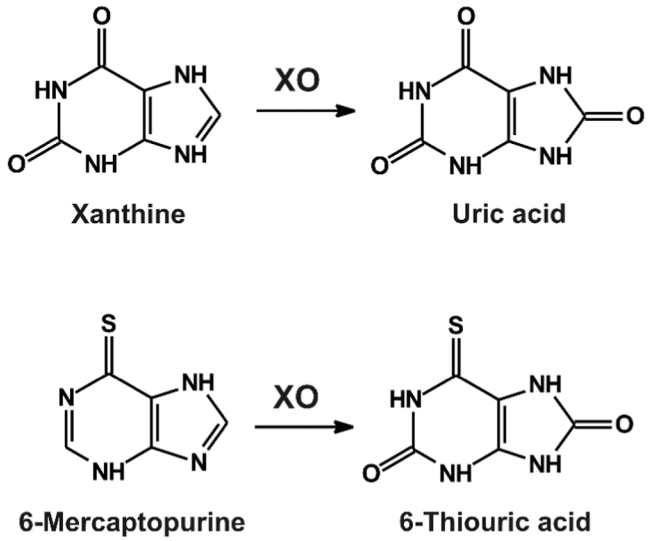

Fig. 2. Xanthine oxidase-catalyzed uric acid and 6-thiouric acid formation.

2. Materials and methods

2.1. Reagents

Luteolin (LUT), naringenin (NAR), xanthine oxidase (XO; from bovine milk), xanthine, uric acid, allopurinol (APU), 6-mercaptopurine (6MP), orthophosphoric acid (ACS reagent, 85% in water), sodium hydroxide (reagent grade, purity: 98%), perchloric acid (ACS reagent, 70% in water), and potassium hydroxide (ACS reagent, purity: 85%) were purchased from Merck (Darmstadt, Germany). Luteolin-3′-*O*-glucuronide (L3′G), luteolin-7-*O*-glucuronide (L7G), naringenin-7-*O*-glucuronide (N7G), and 6-thiouric acid (6-TU) were obtained from Carbosynth (Berkshire, UK). Myricetin (MYR) and ampelopsin (AMP) were from abcr GmbH (Karlsruhe, Germany) and Herb Nutritionals Ltd. (Shanghai, China), respectively. Luteolin-3′-*O*-sulfate (L3′S, containing 10% of the isomer luteolin-4′-*O*-sulfate, overall purity 99%), naringenin-4′-*O*-sulfate (N4′S, 99.6%), myricetin-3′-*O*-sulfate (M3′S, 97.6%) and ampelopsin-4′-*O*-sulfate (A4′S, 97%) were synthesized chemo-enzymatically using arylsulfotransferase from *Desulfitobacterium hafniense* as it has been previously reported [27,28].

Flavonoids were dissolved in dimethyl sulfoxide (DMSO, spectroscopic grade; Fluka, Charlotte, NC, US), then the stock solutions (10 mM each) were stored at −20 °C. The stock solutions of xanthine (1 mM), 6-MP (2 mM), 6-thiouric acid (2 mM), and allopurinol (5 mM) were also prepared in DMSO, while uric acid (2 mM) was dissolved in 0.01 M sodium hydroxide.

2.2. XO assay with xanthine as substrate

Our previously reported method [25] was applied with minor modifications. The incubates (with 500 μL final volume) contained the substrate (xanthine, 5 μM) and the enzyme (XO, 0.0003 U/mL) without or with increasing concentrations of flavonoids (0–50 μM) in sodium phosphate buffer (0.05 M, pH 7.5). Incubations were performed in a thermomixer (8 min, 700 rpm, 37 °C), the reaction was started with the addition of the enzyme. Solvent (DMSO) controls were applied in each experiment, and the impacts of allopurinol (positive control inhibitor) were also tested. The reaction was stopped with 30 μL of perchloric acid solution (6 M), after which samples were vortexed and 195 μL of potassium hydroxide solution (1 M) was added. Thereafter, incubates were cooled to 4 °C, then centrifuged (5 min, 14,000 g, 4 °C). The concentrations of xanthine and uric acid in the supernatants were analyzed by HPLC-UV as has been previously reported [25], without modifications.

2.3. XO assay with 6-MP substrate

We used our previously described method [25] with minor modifications. The incubations were performed in a thermomixer (25 min, 700 rpm, 37 °C), in the presence of the substrate (6-MP, 5 μM) and the enzyme (XO, 0.01 U/mL) without or with increasing concentrations of flavonoids (0–50 μM). Other experimental details were the same as described in Section 2.2. The concentrations of 6-MP and 6-thiouric acid in the supernatants were quantified by HPLC-UV as has been earlier reported [25], without modifications.

2.4. Molecular modeling studies

The structures of LUT, L3′S, L3′G ((2 S,3 S,4 S,5 R,6 S)− 6-[5-(5,7-dihydroxy-4-oxochromen-2-yl)− 2-hydroxyphenoxy]− 3,4,5-trihydroxyoxane-2-carboxylic acid), L7G ((2 S,3 S,4 S,5 R,6 S)− 6-[2-(3,4-dihydroxyphenyl)− 5-hydroxy-4-oxochromen-7-yl]oxy-3,4,5-trihydroxyoxane-2-carboxylic acid), NAR ((2 S)− 5,7-dihydroxy-2-(4-hydroxyphenyl)− 2,3-dihydrochromen-4-one), N4′S, N7G ((2 S,3 S,4 S,5 R,6 S)− 3,4,5-trihydroxy-6-[[5-hydroxy-2-(4-hydroxyphenyl)− 4-oxo-2,3-dihydrochromen-7-yl]oxy]oxane-2-carboxylic acid), MYR, M3′S, AMP ((2 R,3 R)− 3,5,7-trihydroxy-2-(3,4,5-trihydroxyphenyl)− 2,3-dihydrochromen-4-one), and A4′S were built in Maestro (Schrödinger Maestro Schrödinger Release 2020–4). The built structures were further prepared for docking exactly as described in our previous studies [29–31].

Atomic coordinates of XO were obtained from the Protein Data Bank (PDB) with PDB code 3eub [32], according to our previous studies [25,26]. The target was prepared as has been earlier reported [25]. Briefly, non-amino acid molecule molybdopterin and molybdenum complex (MoCo) were subjected to quantum chemical structural optimization and partial charge distribution using MOPAC (Stewart Computational Chemistry, Colorado Springs, CO, US, H. net MOPAC 2016) with a PM7 parametrization [33], and a gradient norm of 0.001. The rest of the target amino acids were equipped with Gasteiger-Marsilli partial charges [34].

Ligands were docked to XO using AutoDock 4.2.6 [35]. The number of grid points were set to 40 × 40 × 40 at a 0.350 Å grid spacing and the center of the grid box was set as the average coordinates (−48.81, 67.55, −43.07) of the experimental binding position of xanthine found in the 3eub PDB structure. Lamarckian genetic algorithm was used for the global search. Ten docking runs were performed for each ligand, and the resulting ligand conformations were ranked by their free energy of binding ($\Delta G_{binding}$) values [36]. The lower rank indicates a more favorable calculated free energy of binding. Representative docked ligand conformations were used for subsequent evaluations [37].

2.5. Data analyses

Figures and tables show means ± standard errors of the mean (SEM) values from three independent experiments. Statistical analyses were carried out ($p < 0.05$ and $p < 0.01$) by one-way ANOVA (with Tukey's post-hoc) test applying the SPSS Statistics software (IBM, Armonk, NY, US).

IC_{50} values were determined based on sigmoidal fitting (Hill1) employing the Origin software (version 2018, OriginLab Corporation, Northampton, MA, US).

3. Results

3.1. Testing the potential inhibitory effects of flavonoids on XO-catalyzed xanthine and 6-MP oxidation

First, the impact of a relatively high flavonoid concentration (20 μM) was examined on XO enzyme with both substrates (xanthine and 6-MP). Among the flavonoids tested, LUT and L3′S almost completely abolished the metabolite formation in both assays (Fig. 3). MYR and M3′S reduced to zero the XO-catalyzed 6-MP oxidation, while they induced weaker impacts on xanthine oxidation. L3′G and L7G strongly decreased XO activity, showing somewhat weaker inhibitory action on xanthine vs. 6-MP oxidation (Fig. 3). NAR, N4′S, and A4′S induced moderate (approximately 40–60%) inhibition, where NAR and A4′S exerted slightly stronger inhibitory effects on xanthine than on 6-MP oxidation. Finally, N7G and AMP did not affect 6-MP oxidation, while they caused the statistically significant ($p < 0.01$) but weak (approximately 20%) inhibition of xanthine oxidation. Based on these observations, we decided to test the concentration dependent inhibitory actions of LUT, L3′S, L3′G, L7G, MYR, and M3′S in the following experiments.

3.2. Concentration dependent effects of LUT, MYR, and their metabolites on XO-catalyzed xanthine oxidation

LUT and L3′S caused significant ($p < 0.01$; 10% and 25% decrease, respectively) inhibition of uric acid formation even at 0.05 μM concentration and induced close to complete inhibition at 20 μM (Fig. 4A). Both LUT ($IC_{50} = 0.21$ μM) and L3′S ($IC_{50} = 0.13$ μM) induced slightly stronger inhibitory actions compared to the positive control allopurinol ($IC_{50} = 0.25$ μM). However, the glucuronide conjugates of LUT showed significant inhibitory effects only at 1 μM concentration (26% and 12% decrease in metabolite formation were caused by L3′G and L7G, respectively), and they proved to be more than tenfold weaker inhibitors of xanthine oxidation than allopurinol (Table 1).

MYR induced statistically significant decrease ($p < 0.01$; 15%) in uric acid formation at 0.1 μM, while M3′S inhibited xanthine oxidation even at 0.01 μM ($p < 0.05$; 8% decrease) and 0.03 μM ($p < 0.01$; 18% decrease) concentrations (Fig. 4B). However, even at 20 μM, MYR and M3′S did not block completely the enzyme, showing approximately 80% and 90% maximal inhibitions, respectively. Nevertheless, based on the IC_{50} values, MYR can be considered as a similarly strong inhibitor of xanthine oxidation than allopurinol (Table 1), while M3'S ($IC_{50} = 0.14$ μM) caused even stronger impact.

3.3. Concentration-dependent effects of LUT, MYR, and their metabolites on XO-catalyzed 6-MP oxidation

Among the compounds tested, L3′S proved to be the strongest inhibitor of 6-MP oxidation ($IC_{50} = 0.13$ μM); it caused statistically significant inhibition ($p < 0.01$; 9% decrease) even at 0.01 μM concentration (Fig. 5A). L3′S was followed by the parent flavonoid LUT ($IC_{50} = 0.34$ μM) with a somewhat weaker effect. Furthermore, both LUT and L3′S caused complete inhibition of the enzyme at 5 μM concentration. Since allopurinol is a much weaker inhibitor of 6-MP oxidation ($IC_{50} = 5.1$ μM) compared with xanthine oxidation ($IC_{50} = 0.25$ μM) (Figs. 4 and 5), LUT and L3′S exerted considerably stronger inhibitory effects on XO-catalyzed 6-thiouric acid formation compared to the positive control. In addition, L3′G and L7G were similarly strong inhibitors as allopurinol, with slightly lower IC_{50} values (Table 1).

Interestingly, MYR and M3′S did not cause the complete inhibition of xanthine oxidation even at 20 μM (Fig. 4B), while MYR and M3′S abolished 6-MP oxidation at 20 μM and 5 μM concentrations, respectively (Fig. 5B). MYR caused the slightly weaker inhibition of 6-thiouric acid formation than allopurinol (Table 1); however, M3′S ($IC_{50} = 0.72$ μM) proved to be considerably stronger inhibitor than MYR and allopurinol (Fig. 5B).

3.4. Molecular modeling studies

The flavonoids were docked into the active site of XO (Fig. 6A), to the binding site of the endogenous substrate xanthine. The flavonoid ring structure shows a well-fit overlap with the xanthine ring (Figs. 6, 7, S1, and S2). Based on the differences between the calculated free energies ($\Delta G_{binding}$), the sulfate metabolites of LUT, NAR, and MYR bind with

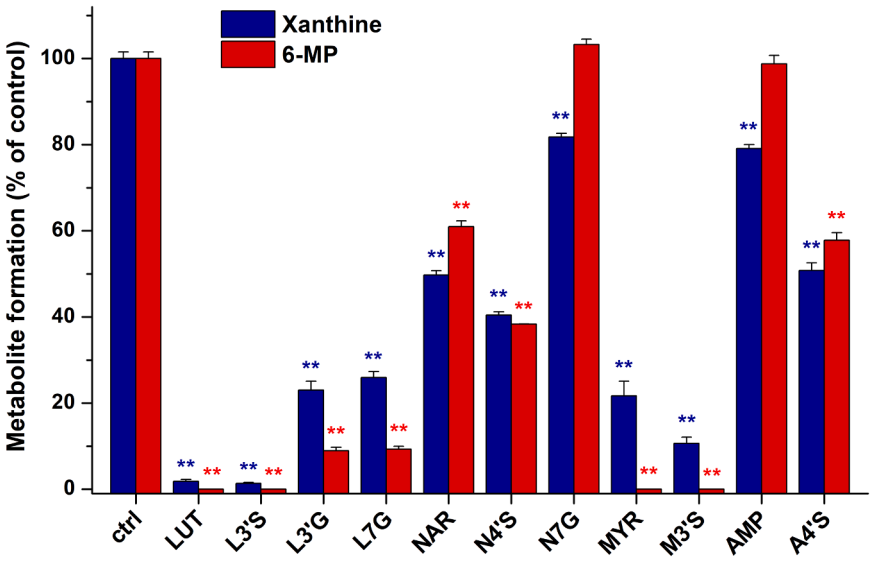

Fig. 3. Effects of flavonoids (20 μM each) on XO-catalyzed xanthine (blue) and 6-MP (red) oxidation (substrate concentrations = 5 μM in both assays; n = 3; *p < 0.05, **p < 0.01). At 20 μM concentration, the positive control inhibitor allopurinol caused almost complete inhibition of metabolite formation (see later in Figs. 4 and 5) in both assays (LUT, luteolin; L3′S, luteolin-3′-*O*-sulfate; L3′G, luteolin-3′-*O*-glucuronide; L7G, luteolin-7-*O*-glucuronide; NAR, naringenin; N4′S, naringenin-4′-*O*-sulfate; N7G, naringenin-7-*O*-glucuronide; MYR, myricetin; M3′S, myricetin-3′-*O*-sulfate; AMP, ampelopsin; A4′S, ampelopsin-4′-*O*-sulfate).

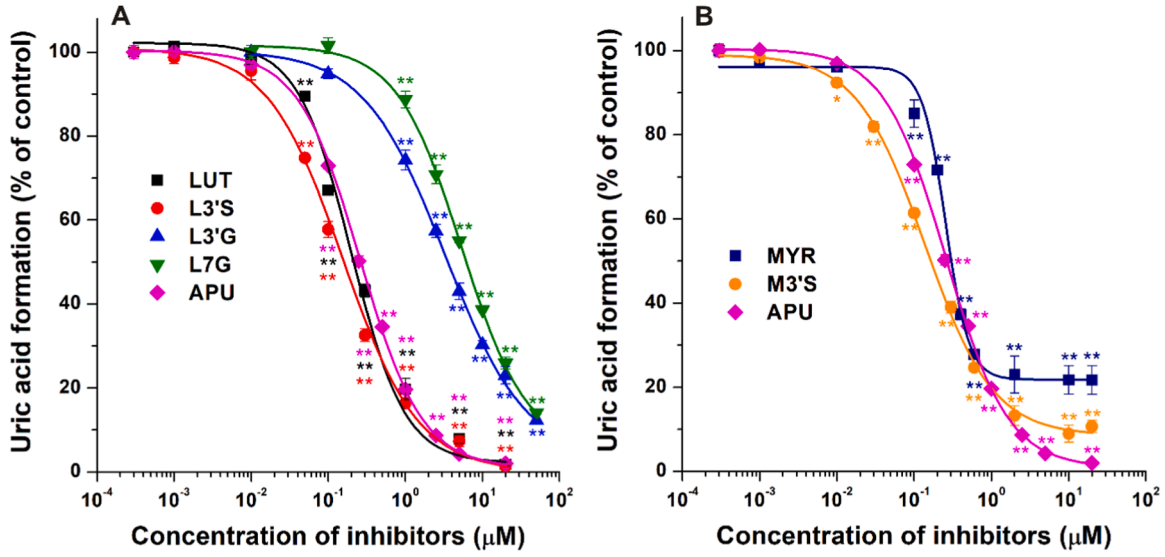

Fig. 4. Concentration dependent inhibitory effects of LUT and its metabolites (A), MYR and its metabolite (B), and allopurinol (APU; positive control; in both panels) on XO-catalyzed xanthine oxidation (substrate concentration = 5 μM; n = 3; *p < 0.05, **p < 0.01; LUT, luteolin; L3′S, luteolin-3′-*O*-sulfate; L3′G, luteolin-3′-*O*-glucuronide; L7G, luteolin-7-*O*-glucuronide; MYR, myricetin; M3′S, myricetin-3′-*O*-sulfate).

Table 1
IC_{50} values of allopurinol, LUT, L3′S, L3′G, L7G, MYR, and M3′S regarding XO-catalyzed xanthine and 6-MP oxidation.

	Xanthine oxidation		6-MP oxidation	
	IC_{50} (μM)	α*	IC_{50} (μM)	α*
Allopurinol (APU)	0.25 ± 0.01	1.00	5.10 ± 0.50	1.00
Luteolin (LUT)	0.21 ± 0.02	0.84	0.34 ± 0.02	0.07
LUT-3′-*O*-sulfate (L3′S)	0.13 ± 0.01	0.52	0.13 ± 0.01	0.03
LUT-3′-*O*-glucuronide (L3′G)	3.22 ± 0.24	12.9	3.00 ± 0.22	0.59
LUT-7-*O*-glucuronide (L7G)	5.20 ± 0.38	20.8	3.93 ± 0.27	0.77
Myricetin (MYR)	0.24 ± 0.01	0.96	3.83 ± 0.08	0.75
MYR-3′-*O*-sulfate (M3′S)	0.14 ± 0.01	0.56	0.72 ± 0.01	0.14

* α = IC_{50} of the flavonoid / IC_{50} of the positive control

higher affinity to the enzyme compared to the respective parent flavonoids, while the comparison of A4′S and AMP showed opposite results (Table 2). Furthermore, modeling studies suggested weaker interactions of glucuronide derivatives (L3′G, L7G, N7G) with XO than their parent flavonoids (Table 2). The interacting amino acids are listed in Table S1.

The greatest difference in $\Delta G_{binding}$ was observed between N4′S and N7G (Table 1). The comparison of their top ranked binding modes (Fig. S1C and D) shows that an oxygen of the sulfate group (which has a partial negative charge) interacts with the central molybdenum (which has a partial positive charge), and the same applies to R880 with its positively charged side chain. The flavonoid rings show a π-stacking interaction with F914 and a hydroxyl group can form a hydrogen bond with S876. The direct interaction of glucuronide metabolites with the molybdenum center is lacking, while the glucuronic acid part interacts through hydrogen bonding with N768, H875, and S876.

4. Discussion

Several in vitro studies demonstrated the potent inhibitory effects of some flavonoid aglycones on XO enzyme [20,22–24]. Due to the extensive presystemic metabolism of flavonoids by sulfotransferase and uridine 5'-diphospho-glucuronosyltransferase enzymes in enterocytes

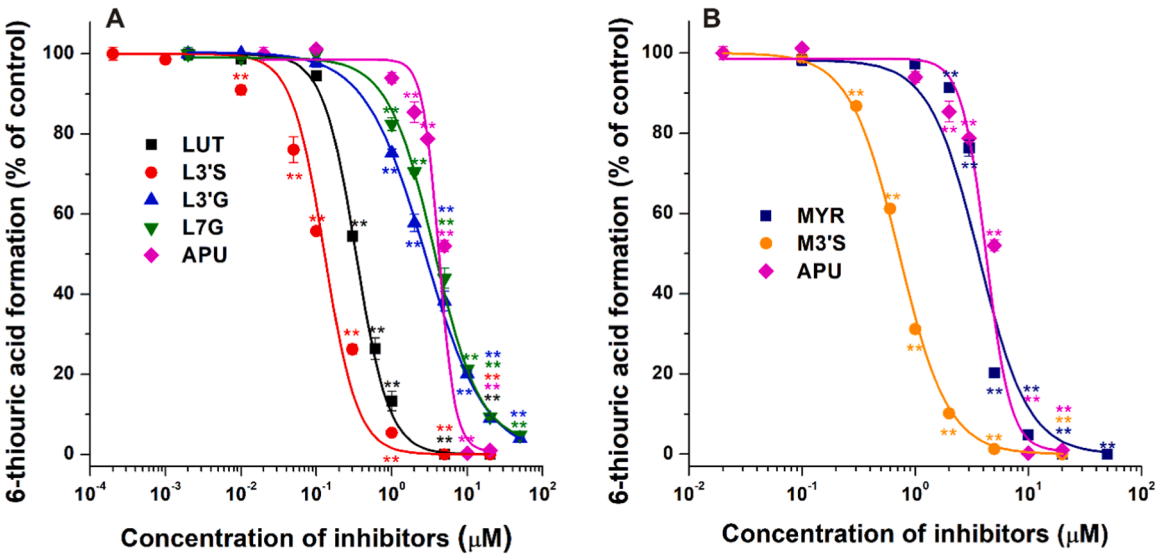

Fig. 5. Concentration dependent inhibitory effects of LUT and its metabolites (A), MYR and its metabolite (B), and allopurinol (APU; positive control; in both panels) on XO-catalyzed 6-MP oxidation (substrate concentration = 5 μM; n = 3; *p < 0.05, **p < 0.01; LUT, luteolin; L3′S, luteolin-3′-*O*-sulfate; L3′G, luteolin-3′-*O*-glucuronide; L7G, luteolin-7-*O*-glucuronide; MYR, myricetin; M3′S, myricetin-3′-*O*-sulfate).

and/or in hepatocytes, typically the sulfate and/or glucuronide metabolites of flavonoids reach high concentrations in the circulation and in certain tissues [1–3]. However, the interactions of these conjugates with the XO enzyme have been barely characterized.

Among the flavonoid aglycones tested, LUT and MYR were strong, NAR was moderate, and AMP was a weak inhibitor of both xanthine and 6-MP oxidations (Fig. 3). These observations are in agreement with previous studies, where LUT and MYR showed strong while NAR and AMP caused much weaker inhibition on XO-catalyzed xanthine oxidation [22–24]. Earlier reports suggest nanomolar IC_{50} values of LUT and low micromolar IC_{50} of MYR [22,23,38]. In the current study, the IC_{50} of LUT and MYR were 0.21 μM and 0.24 μM, respectively. Nevertheless, high concentrations of LUT decreased the uric acid formation close to zero, while MYR did not induce the complete inhibition of xanthine oxidation (the lower plateau of its sigmoid curve was observed between 2 and 20 μM concentrations) (Fig. 4). Interestingly, MYR was a tenfold weaker inhibitor of XO-catalyzed 6-MP oxidation than LUT (Fig. 5 and Table 1).

Regarding LUT, NAR, and MYR, the results of our modeling studies were compared with the previously reported data [39–42]. Docking studies suggested the same interacting amino acids for LUT in another paper [39]. Furthermore, in accordance with the present work (Table 2), an earlier study [40] described similar interaction energies (based on docking scores) of LUT and NAR, and a lower score of MYR. In another study with NAR [40], the same interacting amino acids were highlighted than in the current work (Table S1), with an emphasis on the role of R880. In addition, in two earlier reports [40,41], the same interacting amino acids were found for MYR than in our study (Table S1), also highlighting the important interactions with E802, R880, and E1261. Zhang et al. [42] performed thermodynamic measurements regarding MYR-XO interaction, where the experimental $\Delta G_{binding}$ was − 5.82 kcal/mol (converted from kJ/mol), which perfectly agrees with our $\Delta G_{binding}$ (−5.70 kcal/mol).

Glucuronides were weaker while sulfate conjugates were stronger inhibitors of XO compared to the parent aglycones (Figs. 3–5). Modeling studies were in accordance with these experimental observations, except AMP where the modeling predicted lower affinity interaction with the sulfate derivative (Table 2). Based on earlier reports, quercetin-3-glucuronide and isorhamnetin-3-glucuronide did not affect XO activity [25], and chrysin-7-glucuronide induced only slight inhibition [26]. In the current study, N7G caused slight and no inhibition on xanthine and 6-MP oxidation, respectively (Fig. 3). Surprisingly, both glucuronide metabolites of LUT (L3′G and L7G) proved to be moderate inhibitors of XO ($IC_{50} \approx$ 3–5 μM; Table 1), highlighting that certain glucuronic acid conjugates can also be considered as XO inhibitors. Our previous study with quercetin and quercetin-3′-*O*-sulfate showed that sulfates can be more potent inhibitors of XO [25]. However, as an exception, chrysin-7-*O*-sulfate caused considerably weaker inhibition on XO than chrysin [26]. Considering the above-listed results, we can conclude that the sulfate metabolites of flavonoids are typically stronger inhibitors of XO compared to the parent flavonoid, as it has been noticed based on the comparison of L3′S vs. LUT, N4′S vs. NAR, M3′S vs. MYR, A4′S vs. AMP, and quercetin-3′-*O*-sulfate vs. quercetin.

Generally, in modeling studies, two orientations of the sulfate groups were observed. The first was noticed with L3′S (Fig. 6E) and M3′S (Fig. 7C), where the sulfate groups form hydrogen-bonding interactions with N768 and E802. The respective parent compounds (LUT and MYR) did not show these interactions (Table S1). In the second orientation, the sulfate groups of N4′S (Fig. S1D) and A4′S (Fig. S2C) produce ionic interactions with R880, whereas the parent compounds (NAR and AMP) only form hydrogen-bonds with R880 (Table S1). In addition, N4′S also forms a further hydrogen-bond with E1261 (Fig. S1B).

Most of the flavonoids previously examined exerted similar inhibitory effects on XO regardless of the substrate applied [25,26]. However, certain compounds caused considerably stronger inhibition of xanthine (e.g., pyrogallol and allopurinol) or 6-MP (e.g., 3-phenylpropionic acid and 3-coumaric acid) oxidation [25,26]. In the current study, LUT, L3′S, L3′G, L7G, NAR, N4′S, N7G, AMP, and A4′S showed no differences or induced relatively similar inhibitory effects regarding the two reactions. However, M3′S was 5-fold while MYR was 16-fold stronger inhibitor of xanthine oxidation than 6-MP oxidation (Table 1).

Some studies suggest the potential antihyperuricemic activity of LUT and MYR [43–45]. Even 10 μM concentration of LUT markedly decreased uric acid formation in cultured hepatocytes [43]. In a dose dependent fashion, LUT (20–100 mg/kg/day, *per os* treatment for six days) strongly lowered serum uric acid levels in potassium oxonate-induced hypouricemic mice [44]. Furthermore, in a similar mice experiment, MYR (50–100 mg/kg/day) and LUT (100 mg/kg/day) significantly reduced serum uric acid concentrations (flavonoids were administered perorally for three days) [45]. Our current study highlights that LUT and MYR are similarly strong, while L3′S and M3′S are stronger inhibitors of xanthine oxidation than the positive control allopurinol,

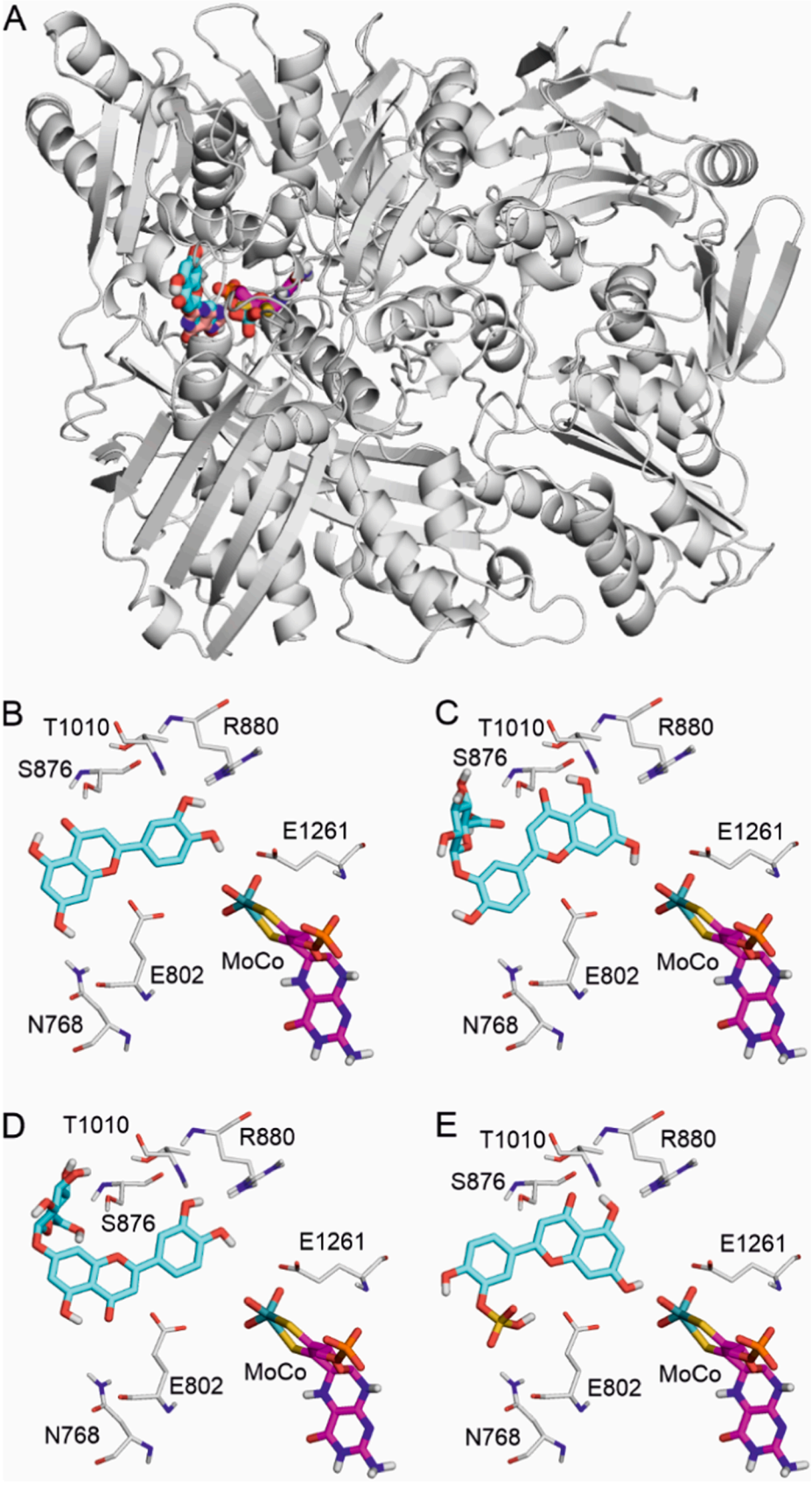

Fig. 6. Binding of xanthine (thick salmon sticks from the 3eub PDB structure) and LUT (thick teal sticks, 1st ranked binding mode) to the XO enzyme (grey cartoon) (A). The molybdenum cofactor (MoCo) is shown as thick purple sticks. The close-up of the binding of LUT (B), L3′G (C), L7G (D), and L3′S (E) are shown in subsequent smaller panels. The flavonoids are represented with teal sticks, and the interacting amino acids (within 3.5 Å distance) are demonstrated as thick grey lines and labeled according to the 3eub PDB structure.

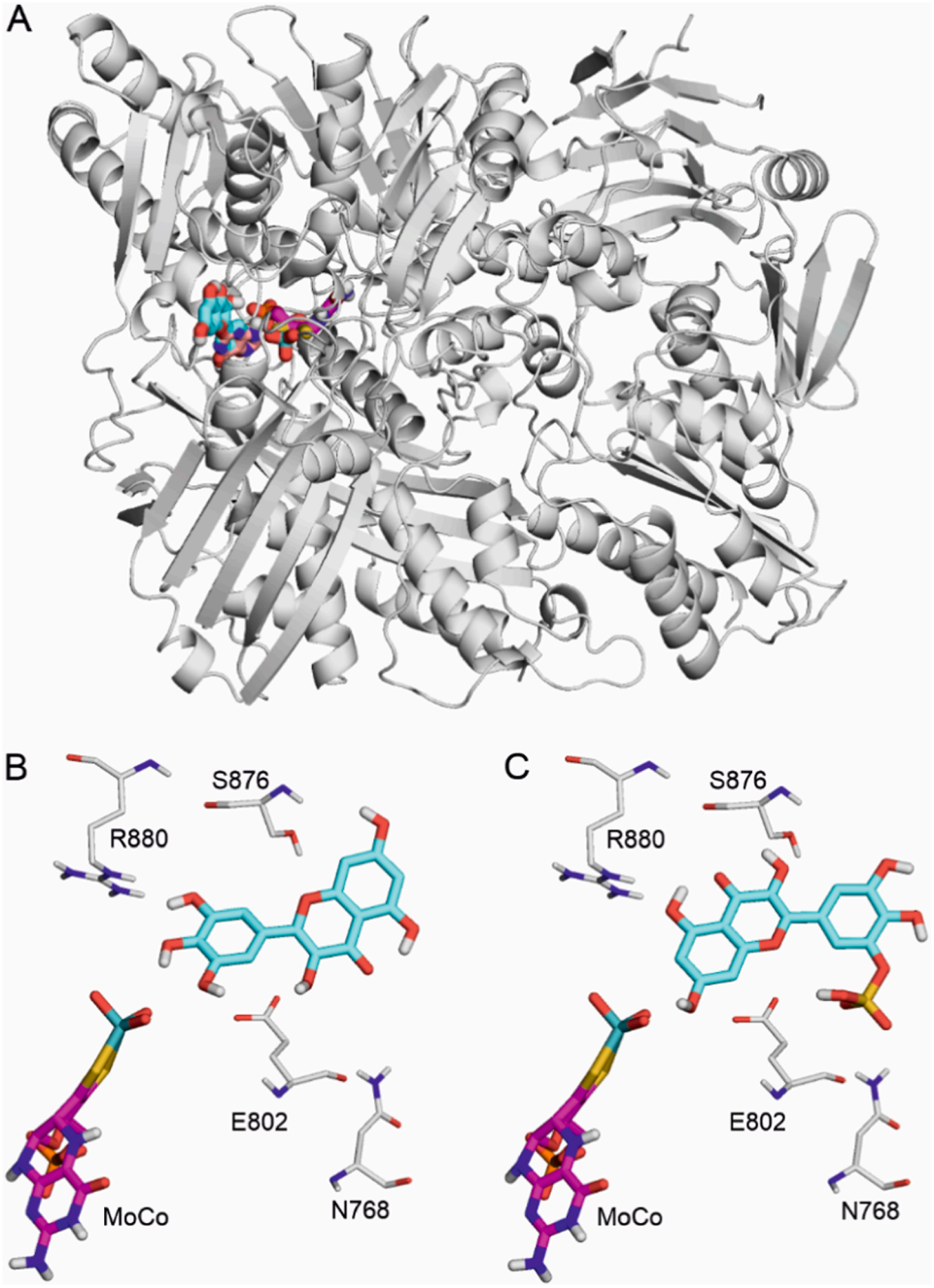

Fig. 7. Binding of xanthine (thick salmon sticks from the 3eub PDB structure) and MYR (thick teal sticks, 1st ranked binding mode) to the XO enzyme (grey cartoon) (A). The molybdenum cofactor (MoCo) is shown as thick purple sticks. The close-up of the binding of MYR (B) and M3′S (C) are shown in subsequent smaller panels. The flavonoids are represented with as teal sticks, and the interacting amino acids (within 3.5 Å distance) are demonstrated as thick grey lines and labeled according to the 3eub PDB structure.

and even the glucuronide conjugates of LUT showed moderate inhibitory effects (Table 1). These data suggest that the conjugated metabolites of these flavonoids may be involved in the previously reported antihyperuricemic impacts of LUT and MYR.

Compared to allopurinol, L3′S, LUT, and M3′S were 40-fold, 15-fold, and 7-fold stronger inhibitors of 6-MP oxidation, respectively (Table 1). Furthermore, L3′G, L7G, and MYR caused slightly stronger inhibition than the positive control (Fig. 5). Allopurinol can disrupt the elimination of 6-MP leading to clinically relevant drug-drug interaction [21]. Therefore, to explore their clinical importance, the in vivo investigation of the potential pharmacokinetic interactions of LUT and MYR with 6-MP and/or azathioprine are highly reasonable.

5. Conclusions

In summary, the inhibitory effects of LUT, L3′S, L3′G, L7G, NAR, N4′S, N7G, MYR, M3′S, AMP, and A4′S were examined on XO-catalyzed xanthine and 6-MP oxidations using in vitro enzyme assays. Furthermore, flavonoid-XO interactions were also studied applying molecular modeling technique. Our results demonstrate that sulfation increased the inhibitory potency of LUT, NAR, MYR, and AMP on XO enzyme regarding both substrates tested. In addition, LUT, MYR, and their sulfates proved to be strong inhibitors of the enzyme, even compared to the positive control allopurinol. Glucuronidation of LUT and NAR resulted in less potent inhibitors; however, low micromolar concentrations of L3′G and L7G caused relevant decreases in metabolite formation. Flavonoids showed similar inhibitory effects in the presence of both substrates, except MYR and M3′S exerted stronger inhibitory actions on xanthine oxidation than on 6-MP oxidation. Considering their high inhibitory potency, the conjugated metabolites of LUT and MYR can take part in the inhibitory actions of these flavonoids on XO enzyme.

Table 2
The calculated free energies of binding ($\Delta G_{binding}$) regarding flavonoid-XO interactions examined.

Flavonoid	$\Delta G_{binding}$ (kcal/mol)	Binding rank/all ranks
Luteolin (LUT)	–6.23	1/2
LUT-3′-*O*-sulfate (L3′S)	–7.64	1/2
LUT-3′-*O*-glucuronide (L3′G)	–5.67	1/3
LUT-7-*O*-glucuronide (L7G)	–3.67	1/4
Naringenin (NAR)	–6.22	1/2
NAR-4′-*O*-sulfate (N4′S)	–7.83	1/2
Naringenin-7-*O*-glucuronide (N7G)	–3.41	1/4
Myricetin (MYR)	–5.70	1/2
MYR-3′-*O*-sulfate (M3′S)	–6.70	1/2
Ampelopsin (AMP)	–5.87	1/1
AMP-4′-*O*-sulfate (A4′S)	–5.05	1/2

Funding

The work of M.P. is supported by the Hungarian National Research, Development and Innovation Office (FK138184) and by the János Bolyai Research Scholarship of the Hungarian Academy of Sciences (BO/00381/21). K.V. was supported by Czech Science Foundation (23-04654S). The project has been supported the PTE ÁOK KA-2022-26 grant, and by the European Union, co-financed by the European Social Fund (project name and code: Comprehensive Development for Implementing Smart Specialization Strategies at the University of Pécs, EFOP-3.6.1-16-2016-00004).

CRediT authorship contribution statement

Orsolya Balázs: Formal analysis, Investigation, Writing – original draft; **Ágnes Dombi:** Formal analysis, Investigation. **Balázs Z. Zsidó:** Formal analysis, Investigation; **Csaba Hetényi:** Funding acquisition, Investigation, Methodology, Supervision, Validation, Writing – original draft; **Kateřina Valentová:** Funding acquisition, Methodology, Validation; **Róbert G. Vida:** Conceptualization; **Miklós Poór:** Conceptualization, Funding acquisition, Investigation, Methodology, Supervision, Validation, Writing – original draft.

Declaration of Competing Interest

The authors declare no competing interests.

Acknowledgements

The authors thank Katalin Fábián and Dóra Bense for their excellent assistance in the experimental work. We acknowledge the support from the Governmental Information Technology Development Agency, Hungary. We acknowledge that the results of this research have been achieved using the DECI resource Archer2 based in the UK at the National Supercomputing Service with support from the PRACE aisbl.

Appendix A. Supporting information

Supplementary data associated with this article can be found in the online version at doi:10.1016/j.biopha.2023.115548.

References

[1] J.A. Ross, C.M. Kasum, Dietary flavonoids: bioavailability, metabolic effects, and safety, Annu. Rev. Nutr. 22 (2002) 19–34, https://doi.org/10.1146/annurev.nutr.22.111401.144957.
[2] A. Naeem, Y. Ming, H. Pengyi, K.Y. Jie, L. Yali, Z. Haiyan, X. Shuai, L. Wenjing, W. Ling, Z.M. Xia, L.S. Shan, Z. Qin, The fate of flavonoids after oral administration: a comprehensive overview of its bioavailability, Crit. Rev. Food Sci. Nutr. 62 (2022) 6169–6186, https://doi.org/10.1080/10408398.2021.1898333.
[3] S.H. Thilakarathna, H.P.V. Rupasinghe, Flavonoid bioavailability and attempts for bioavailability enhancement, Nutrients 5 (2013) 3367–3387, https://doi.org/10.3390/nu5093367.
[4] J. Zhao, J. Yang, Y. Xie, Improvement strategies for the oral bioavailability of poorly water-soluble flavonoids: an overview, Int. J. Pharm. 570 (2019), 118642, https://doi.org/10.1016/j.ijpharm.2019.118642.
[5] S.M. Wittemer, M. Ploch, T. Windeck, S.C. Müller, B. Drewelow, H. Derendorf, M. Veit, Bioavailability and pharmacokinetics of caffeoylquinic acids and flavonoids after oral administration of Artichoke leaf extracts in humans, Phytomedicine 12 (2005) 28–38, https://doi.org/10.1016/j.phymed.2003.11.002.
[6] Y. Taheri, J. Sharifi-Rad, G. Antika, Y.B. Yılmaz, T.B. Tumer, S. Abuhamdah, S. Chandra, S. Saklani, C.S. Kılıç, S. Sestito, S.D. Daştan, M. Kumar, M.M. Alshehri, S. Rapposelli, N. Cruz-Martins, W.C. Cho, Paving luteolin therapeutic potentialities and agro-food-pharma applications: emphasis on in vivo pharmacological effects and bioavailability traits, Oxid. Med. Cell. Longev. 2021 (2021) 1–20, https://doi.org/10.1155/2021/1987588.
[7] N. Hayasaka, N. Shimizu, T. Komoda, S. Mohri, T. Tsushida, T. Eitsuka, T. Miyazawa, K. Nakagawa, Absorption and metabolism of luteolin in rats and humans in relation to in vitro anti-inflammatory effects, J. Agric. Food Chem. 66 (2018) 11320–11329, https://doi.org/10.1021/acs.jafc.8b03273.
[8] R. Joshi, Y.A. Kulkarni, S. Wairkar, Pharmacokinetic, pharmacodynamic and formulations aspects of Naringenin: An update, Life Sci. 215 (2018) 43–56, https://doi.org/10.1016/j.lfs.2018.10.066.
[9] J. Zhang, J.S. Brodbelt, Screening flavonoid metabolites of naringin and narirutin in urine after human consumption of grapefruit juice by LC-MS and LC-MS/MS, Analyst 129 (2004) 1227, https://doi.org/10.1039/b412577k.
[10] I. Erlund, E. Meririnne, G. Alfthan, A. Aro, Plasma kinetics and urinary excretion of the flavanones naringenin and hesperetin in humans after ingestion of orange juice and grapefruit juice, J. Nutr. 131 (2001) 235–241, https://doi.org/10.1093/jn/131.2.235.
[11] C.J. Rebello, R.A. Beyl, J.J.L. Lertora, F.L. Greenway, E. Ravussin, D.M. Ribnicky, A. Poulev, B.J. Kennedy, H.F. Castro, S.R. Campagna, A.A. Coulter, L.M. Redman, Safety and pharmacokinetics of naringenin: a randomized, controlled, single-ascending-dose clinical trial, Diabetes Obes. Metab. 22 (2020) 91–98, https://doi.org/10.1111/dom.13868.
[12] S.P. Lin, Y.C. Hou, S.Y. Tsai, M.J. Wang, P.D.L. Chao, Tissue distribution of naringenin conjugated metabolites following repeated dosing of naringin to rats, BioMedicine 4 (2014) 16, https://doi.org/10.7603/s40681-014-0016-z.
[13] Y. Dang, G. Lin, Y. Xie, J. Duan, P. Ma, G. Li, G. Ji, Quantitative determination of myricetin in rat plasma by ultra performance liquid chromatography tandem mass spectrometry and its absolute bioavailability, Drug. Res. 64 (2014) 516–522, https://doi.org/10.1055/s-0033-1363220.
[14] L. Liu, X. Yin, X. Wang, X. Li, Determination of dihydromyricetin in rat plasma by LC-MS/MS and its application to a pharmacokinetic study, Pharm. Biol. 55 (2017) 657–662, https://doi.org/10.1080/13880209.2016.1266669.
[15] J. Zhou, P. Zeng, H.H. Tu, F.Q. Wang, Development and application of high-performance liquid chromatography for the study of ampelopsin pharmacokinetics in rat plasma using cloud-point extraction, J. Sep. Sci. 34 (2011) 160–168, https://doi.org/10.1002/jssc.201000382.
[16] Q. Tong, X. Hou, J. Fang, W. Wang, W. Xiong, X. Liu, X. Xie, C. Shi, Determination of dihydromyricetin in rat plasma by LC–MS/MS and its application to a pharmacokinetic study, J. Pharm. Biomed. Anal. 114 (2015) 455–461, https://doi.org/10.1016/j.jpba.2015.06.030.
[17] R. Harrison, Structure and function of xanthine oxidoreductase: where are we now, Free Radic. Biol. Med. 33 (2002) 774–797, https://doi.org/10.1016/s0891-5849(02)00956-5.
[18] H.M. Schmidt, E.E. Kelley, A.C. Straub, The impact of xanthine oxidase (XO) on hemolytic diseases, Redox Biol. 21 (2019), 101072, https://doi.org/10.1016/j.redox.2018.101072.
[19] C. Mottet, A.M. Schoepfer, P. Juillerat, J. Cosnes, F. Froehlich, V. Kessler-Brondolo, F. Seibold, G. Rogler, S.R. Vavricka, P. Michetti, Experts opinion on the practical use of azathioprine and 6-mercaptopurine in inflammatory bowel disease, Inflamm. Bowel Dis. 22 (2016) 2733–2747, https://doi.org/10.1097/MIB.0000000000000923.
[20] A. Mehmood, M. Ishaq, L. Zhao, B. Safdar, A. Rehman, M. Munir, A. Raza, M. Nadeem, W. Iqbal, C. Wang, Natural compounds with xanthine oxidase inhibitory activity: a review, Chem. Biol. Drug. Des. 93 (2019) 387–418, https://doi.org/10.1111/cbdd.13437.
[21] H.L. McLeod, Clinically relevant drug-drug interactions in oncology, Br. J. Clin. Pharm. 45 (1998) 539–544, https://doi.org/10.1046/j.1365-2125.1998.00719.x.
[22] P. Cos, L. Ying, M. Calomme, J.P. Hu, K. Cimanga, B. Van Poel, L. Pieters, A. J. Vlietinck, D. Vanden Berghe, Structure-activity relationship and classification of flavonoids as inhibitors of xanthine oxidase and superoxide scavengers, J. Nat. Prod. 61 (1998) 71–76, https://doi.org/10.1021/np970237h.
[23] A. Nagao, M. Seki, H. Kobayashi, Inhibition of xanthine oxidase by flavonoids, Biosci. Biotechnol. Biochem. 63 (1999) 1787–1790, https://doi.org/10.1271/bbb.63.1787.
[24] M. Yuan, Y. Liu, A. Xiao, J. Leng, L. Liao, L. Ma, L. Liu, The interaction of dietary flavonoids with xanthine oxidase in vitro: molecular property-binding affinity relationship aspects, RSC Adv. 9 (2019) 10781–10788, https://doi.org/10.1039/c8ra09926j.
[25] V. Mohos, A. Pánovics, E. Fliszár-Nyúl, G. Schilli, C. Hetényi, P. Mladěnka, P. W. Needs, P.A. Kroon, G. Pethő, M. Poór, Inhibitory effects of quercetin and its human and microbial metabolites on xanthine oxidase enzyme, Int. J. Mol. Sci. 20 (2019) 2681, https://doi.org/10.3390/ijms20112681.

[26] V. Mohos, E. Fliszár-Nyúl, M. Poór, Inhibition of xanthine oxidase-catalyzed xanthine and 6-mercaptopurine oxidation by flavonoid aglycones and some of their conjugates, Int. J. Mol. Sci. 21 (2020) 3256, https://doi.org/10.3390/ijms21093256.
[27] K. Káňová, L. Petrásková, H. Pelantová, Z. Rybková, K. Malachová, J. Cvačka, V. Křen, K. Valentová, Sulfated metabolites of luteolin, myricetin, and ampelopsin: chemoenzymatic preparation and biophysical properties, J. Agric. Food Chem. 68 (2020) 11197–11206, https://doi.org/10.1021/acs.jafc.0c03997.
[28] H. Kaci, S. Bodnárová, E. Fliszár-Nyúl, B. Lemli, H. Pelantová, K. Valentová, É. Bakos, C. Özvegy-Laczka, M. Poór, Interaction of luteolin, naringenin, and their sulfate and glucuronide conjugates with human serum albumin, cytochrome P450 (CYP2C9, CYP2C19, and CYP3A4) enzymes and organic anion transporting polypeptide (OATP1B1 and OATP2B1) transporters, Biomed. Pharmacother. 157 (2023), 114078, https://doi.org/10.1016/j.biopha.2022.114078.
[29] O. Balázs, Á. Dombi, B.Z. Zsidó, C. Hetényi, R.G. Vida, M. Poór, Probing the interactions of 31 mycotoxins with xanthine oxidase: alternariol, alternariol-3-sulfate, and α-zearalenol are allosteric inhibitors of the enzyme, Toxins 15 (2023) 250, https://doi.org/10.3390/toxins15040250.
[30] V. Mohos, E. Fliszár-Nyúl, B. Lemli, B.Z. Zsidó, C. Hetényi, P. Mladěnka, P. Horký, M. Pour, M. Poór, Testing the pharmacokinetic interactions of 24 colonic flavonoid metabolites with human serum albumin and cytochrome P450 enzymes, Biomolecules 10 (2020) 409, https://doi.org/10.3390/biom10030409.
[31] Z. Csenki, T. Bartók, I. Bock, L. Horváth, B. Lemli, B.Z. Zsidó, C. Angeli, C. Hetényi, I. Szabó, B. Urbányi, M. Kovács, M. Poór, Interaction of fumonisin B1, N-palmitoyl-fumonisin B1, 5-O-palmitoyl-fumonisin B1, and fumonisin B4 mycotoxins with human serum albumin and their toxic impacts on zebrafish embryos, Biomolecules 13 (2023) 755, https://doi.org/10.3390/biom13050755.
[32] J.M. Pauff, H. Cao, R. Hille, Substrate orientation and catalysis at the molybdenum site in xanthine oxidase, J. Biol. Chem. 284 (2009) 8760–8767, https://doi.org/10.1074/jbc.M804517200.
[33] J.J.P. Stewart, Optimization of parameters for semiempirical methods VI: more modifications to the NDDO approximations and Re-optimization of parameters, J. Mol. Model. 19 (2013) 1–32, https://doi.org/10.1007/s00894-012-1667-x.
[34] J. Gasteiger, M. Marsili, Iterative partial equalization of orbital electronegativity – a rapid access to atomic charges, Tetrahedron 36 (1980) 3219–3228, https://doi.org/10.1016/0040-4020(80)80168-2.
[35] G.M. Morris, D.S. Goodsell, R.S. Halliday, R. Huey, W.E. Hart, R.K. Belew, A. J. Olson, Automated docking using a lamarckian genetic algorithm and empirical binding, Free Energy Funct., J. Comput. Chem. 19 (1998) 1639–1662, https://doi.org/10.1002/(SICI)1096-987X(19981115)19:14<1639::AID-JCC10>3.0.CO;2-B.
[36] B.Z. Zsidó, R. Börzsei, V. Szél, C. Hetényi, Determination of ligand binding modes in hydrated viral ion channels to foster drug design and repositioning, J. Chem. Inf. Model. 61 (2021) 4011–4022, https://doi.org/10.1021/acs.jcim.1c00488.
[37] B.Z. Zsidó, M. Balog, N. Erős, M. Poór, V. Mohos, E. Fliszár-Nyúl, C. Hetényi, M. Nagane, K. Hideg, T. Kálai, B. Bognár, Synthesis of spin-labelled bergamottin: a potent CYP3A4 inhibitor with antiproliferative activity, Int. J. Mol. Sci. 21 (2020) 508, https://doi.org/10.3390/ijms21020508.
[38] D.E.C. Van Hoorn, R.J. Nijveldt, P.A.M. Van Leeuwen, Z. Hofman, L. M'Rabet, D.B. A. De Bont, K. Van Norren, Accurate prediction of xanthine oxidase inhibition based on the structure of flavonoids, Eur. J. Pharmacol. 451 (2002) 111–118, https://doi.org/10.1016/s0014-2999(02)02192-1.
[39] J. Yan, G. Zhang, Y. Hu, Y. Ma, Effect of luteolin on xanthine oxidase: inhibition kinetics and interaction mechanism merging with docking simulation, Food Chem. 141 (2013) 3766–3773, https://doi.org/10.1016/j.foodchem.2013.06.092.
[40] D.S. Ghallab, E. Shawky, A.M. Metwally, I. Celik, R.S. Ibrahim, M.M. Mohyeldin, Integrated in silico – in vitro strategy for the discovery of potential xanthine oxidase inhibitors from egyptian propolis and their synergistic effect with allopurinol and febuxostat, RSC Adv. 12 (2022) 2843–2872, https://doi.org/10.1039/D1RA08011C.
[41] C.M. Lin, C.S. Chen, C.T. Chen, Y.C. Liang, J.K. Lin, Molecular modeling of flavonoids that inhibits xanthine oxidase, Biochem. Biophys. Res. Commun. 294 (2002) 167–172, https://doi.org/10.1016/S0006-291X(02)00442-4.
[42] C. Zhang, G. Zhang, Y. Liao, D. Gong, Myricetin inhibits the generation of superoxide anion by reduced form of xanthine oxidase, Food Chem. 221 (2017) 1569–1577, https://doi.org/10.1016/j.foodchem.2016.10.136.
[43] S. Adachi, M. Oyama, S. Kondo, K. Yagasaki, Comparative effects of quercetin, luteolin, apigenin and their related polyphenols on uric acid production in cultured hepatocytes and suppression of purine bodies-induced hyperuricemia by rutin in mice, Cytotechnology 73 (2021) 343–351, https://doi.org/10.1007/s10616-021-00452-9.
[44] Y. Lin, P. Liu, W. Liang, Y. Hu, P. Xu, J. Zhou, J. Pu, H. Zhang, Luteolin-4'-O-glucoside and its aglycone, two major flavones of Gnaphalium affine D. Don, resist hyperuricemia and acute gouty arthritis activity in animal models, Phytomedicine 41 (2018) 54–61, https://doi.org/10.1016/j.phymed.2018.02.002.
[45] S. Mo, F. Zhou, Y. Lv, Q. Hu, D. Zhang, L. Kong, Hypouricemic action of selected flavonoids in mice: structure-activity relationships, Biol. Pharm. Bull. 30 (2007) 1551–1556, https://doi.org/10.1248/bpb.30.1551.